Smart Structures and Systems, *Vol. 18, No. 6 (2016) 1087-1109*
DOI: http://dx.doi.org/10.12989/sss.2016.18.6.1087

Thermal effects on nonlocal vibrational characteristics of nanobeams with non-ideal boundary conditions

Farzad Ebrahimi* and Gholam Reza Shaghaghi

Department of Mechanical Engineering, Faculty of Engineering, Imam Khomeini International University, Qazvin, Iran

(Received May 17, 2015, Revised April 28, 2016, Accepted April 30, 2016)

Abstract. In this manuscript, the small scale and thermal effects on vibration behavior of preloaded nanobeams with non-ideal boundary conditions are investigated. The boundary conditions are assumed to allow small deflections and moments and the concept of non-ideal boundary conditions is applied to the nonlocal beam problem. Governing equations are derived through Hamilton's principle and then are solved applying Lindstedt-Poincare technique to derive fundamental natural frequencies. The good agreement between the results of this research and those available in literature validated the presented approach. The influence of various parameters including nonlocal parameter, thermal effect, perturbation parameter, aspect ratio and pre-stress load on free vibration behavior of the nanobeams are discussed in details.

Keywords: small scale effect; nonlocal beam theory; non-ideal boundary conditions; vibration; thermal effect; preload parameter; perturbation parameter

1. Introduction

In the problems of mechanical systems the boundary conditions (B.Cs) of the structures play a very important role and are usually represented in an idealized form such as clamped, simply supported and free boundary conditions. It is always assumed that those ideal B.Cs are satisfied exactly in the process of the problem solution. Indeed, however small, deviations from the ideal B.Cs may exist and the ideal B.C assumptions sometimes lead to unsatisfactory solutions especially in micro/nano-electro-mechanical systems (MEMs/NEMs). The types of B.Cs with small deviations from the ideal B.Cs are referred as the non-ideal B.Cs which can be modeled via perturbation theory.

The linear vibration problem of a beam for different B.Cs and also an axially moving string problem with simply supported B.Cs have been investigated by Pakdemirli and Boyac (2003). The Euler–Bernoulli beam theory (EBT) with simply supported stable-end conditions and a non-ideal simple support in between was investigated by multiple scales method and perturbation theory. They also studied the nonlinear vibration problem of a beam subjected to tensile loading with non-ideal B.Cs (Pakdemirli and Boyac 2001). Peddieson, Buchanan *et al*. (2003) employed nonlocal elasticity theory and EBT to illustrate the magnitude of predicted nonlocal effects. In

*Corresponding author, Professor, E-mail: febrahimy@eng.ikiu.ac.ir

http://www.techno-press.org/?journal=sss&subpage=8 ISSN: 1738-1584 (Print), 1738-1991 (Online)

other work the problem of damped forced nonlinear vibration of an Euler-Bernoulli beam with non-ideal B.Cs was studied using the method of multiple scales (Ekici and Boyaci 2007). Next, buckling and vibration analysis of a rectangular isotropic plate with non-ideal simply supported B.Cs along one of its edges was investigated by Aydogdu and Ece (2006). They also investigated the effects of non-ideal B.Cs on the vibrations of microbeams while considering the stretching effect as well as axial forces (Ekici and Boyaci, 2007). The effect of non-ideal B.Cs and initial stresses on the vibration of laminated plates resting on Pasternak foundation was studied by Malekzadeh, Khalili *et al.* (2010). Eigoli and Ahmadian (2011) investigated the influence of non-ideal B.Cs on the nonlinear vibration of damped beams subjected to harmonic loads. Sari and Pakdemirli (2012) proposed a new numerical technique for the free vibration analysis of non-rotating and rotating Timoshenko beams with damaged boundaries. For this purpose, the Chebyshev collocation method is applied to obtain the natural frequencies and mode shapes and the damaged boundaries of the Timoshenko beam were represented by distributed translational and torsional springs. Recently Wattanasakulpong and Mao (2015) investigated the dynamic response of Timoshenko beams made of functionally graded materials (FGMs). The beams were supported by various classical and non-classical B.Cs.

Furthermore, in recent years due to superior properties, nanostructures have attracted much attention. Multiple recent experimental results have shown that as the size of the structures reduces to micro/nanoscale, the influences of atomic forces and small scale play a significant role in mechanical properties of these nanostructures (Ebrahimi and Salari 2015 a, b). Thus, neglecting these effects in some cases may result in completely incorrect solutions and hence wrong designs. The classical continuum theories do not include any internal length scale. Consequently, these theories are expected to fail when the size of the structure becomes comparable with the internal length scale. Eringen nonlocal theory is one of the well-known continuum mechanics theories that include small scale effects with good accuracy to model micro/nanoscale devises (Eringen 1972). The nonlocal elasticity theory assumes that the stress at a point is a function of the strain at all neighbor points of the body, hence, this theory could take into account the effects of small scales.

The studies of nanostructures using the nonlocal elasticity theory have been an area of active research. Based on this theory, wave propagation in carbon nanotubes (CNTs) is studied based on nonlocal EBT and Timoshenko beam theories by Wang (2005). In similar work, the scale effects on transverse wave propagation in double-walled carbon nanotubes is studied via nonlocal elasticity theory (Wang, Zhou *et al*. 2006). Also Zhang, Liu *et al.* (2004) studied thermal effect on vibration of double-walled CNTs based on thermal elasticity mechanics and nonlocal elasticity theory. Wang, Ni *et al.* (2008) exploited the thermal effect on vibration and instability of conveying fluid CNTs based on Euler-Bernoulli beam theory. Zhang and Shen (2007) reported the buckling and post buckling behavior of CNTs in thermal environment by using molecular dynamics simulations. Next, bending, buckling and free vibration of nanobeams including different beam theories is investigated by Aydogdu (2009). Murmu and Pradhan (2009) analyzed the thermal vibration of CNTs based on thermal elasticity and nonlocal elasticity theory. Also Benzair, Tounsi *et al.* (2008) employed nonlocal Timoshenko beam model for free vibration analysis of CNTs including thermal effects. Civalek and Demir (2011a) used nonlocal theory for bending analysis of microtubules based on Euler-Bernoulli beam theory. Vibration and bending analysis of cantilever microtubules is studied by Civalek, Demir *et al.* (2010). In similar work, buckling analysis of cantilever CNT is investigated by Civalek and Demir (2011b).

Also, based on nonlocal elasticity theory an elastic Bernoulli–Euler beam model is developed for thermal–mechanical vibration and buckling instability of a single-walled CNT conveying fluid and resting on an elastic medium (Chang 2012). Ansari and Sahmani (2012) studied the nonlinear vibration behavior of CNTs using various beam theories. Thai (2012) studied bending, buckling and vibration of nanobeams.

Size-effects on torsional and axial response of microtubules by using the nonlocal continuum rod model is investigated via finite element method (Demir and Civalek 2013). Bending and buckling behavior of size-dependent nanobeams made of FGMs including the thickness stretching effect has been studied by Mahmoud, Chaht *et al*. (2015). Zemri, Houari *et al*. (2015) presented a nonlocal shear deformation beam theory for bending, buckling, and vibration of functionally graded (FG) nanobeams using the nonlocal differential constitutive relations of Eringen. The nonlinear vibration properties of an embedded zigzag CNT on Winkler foundation are investigated by Besseghier, Heireche *et al*. (2015). Recently Bounouara, Benrahou *et al*. (2016) presented a zeroth-order shear deformation theory for free vibration analysis of FGM nanoscale plates resting on elastic foundation. A refined trigonometric shear deformation theory taking into account the transverse shear deformation effects is presented by Tounsi (2013) for thermoelastic bending analysis of FG sandwich plates. Bouderba, Houari *et al*. (2013) investigated the thermomechanical bending response of FG plates resting on Winkler-Pasternak elastic foundations. The bending response of FG plate resting on elastic foundation and subjected to hygro-thermo-mechanical loading is studied by Zidi et al (2014). It is worth mentioning that in most of the published papers the boundary conditions has been assumed to be ideal (Belabed, Houari *et al*. 2014, Bennoun, Houari *et al*. 2016, Hamidi, Houari e*t al*. 2015, Hebali, Tounsi *et al*. 2014, Tounsi, Bourada *et al*. 2015, Yahia, Atmane *et al*. 2015) and to the best knowledge of the authors, no research effort has been devoted so far to find the solution of thermo-mechanical vibration behavior of nanobeams with non-ideal boundary conditions. In the present study, the EBT is employed based on Eringen's nonlocal elasticity theory to consider the size-effect and thermal effect on free vibration behavior of nanobeams subjected to a pre-stress load. Lindstedt–Poincare technique is utilized to determine natural frequencies of nanobeams and the influences of the nonlocal parameter, perturbation parameter, thermal effect, aspect ratio and pre-stress load on the free vibration characteristics of the nanobeams are discussed in details.

2. Basic formulation

2.1 Nonlocal elasticity theory

The constitutive equation of classical elasticity is an algebraic relationship between the stress and strain tensors while that of Eringen's nonlocal elasticity involves spatial integrals which represent weighted averages of the contributions of strain tensors of all points in the body to the stress tensor at the given point (Eringen 1972). Though it is difficult mathematically to obtain the solution of nonlocal elasticity problems due to the spatial integrals in constitutive equations, these integro-partial constitutive differential equations can be converted to equivalent differential constitutive equations under certain conditions.

The theory of nonlocal elasticity, developed by Eringen and Edelen (1972) states that the nonlocal stress-tensor components σ_{ij} at any point *x* in a body can be expressed as

$$\sigma_{ij}(x) = \int_{\Omega} \alpha(|x' - x|, \tau)\, t_{ij}(x') d\Omega(x') \tag{1}$$

where $t_{ij}(x')$ are the components of the classical local stress tensor at point x, which are related to the components of the linear strain tensor ε_{kl} by the conventional constitutive relations for a Hookean material, i.e.

$$t_{ij} = C_{ijkl}\varepsilon_{kl} \tag{2}$$

The meaning of Eq. (1) is that the nonlocal stress at point *x* is the weighted average of the local stress of all points in the neighborhood of *x*, the size of which is related to the nonlocal Kernel $\alpha(|x'-x|,\tau)$. Here $|x'-x|$ is the Euclidean distance and τ is a constant given by

$$\tau = \frac{e_0 a}{l} \tag{3}$$

which represents the ratio between a characteristic internal length, a (such as lattice parameter, C–C bond length and granular distance) and a characteristic external one, *l* (e.g., crack length, wavelength) through an adjusting constant, e_0 , dependent on each material. The magnitude of e_0 is determined experimentally or approximated by matching the dispersion curves of plane waves with those of atomic lattice dynamics. According to Ref. (Eringen and Edelen 1972) for a class of physically admissible kernel $\alpha(|x'-x|,\tau)$ it is possible to represent the integral constitutive relations given by Eq. (1) in an equivalent differential form as

$$(1-(e_0 a)\nabla^2)\sigma_{kl} = t_{kl} \tag{4}$$

where ∇^2 is the Laplacian operator. Thus, the scale length $e_0 a$ takes into account the size effect on the response of nanostructures. For an elastic material in the one dimensional case, the nonlocal constitutive relations may be simplified as (Eringen 2002)

$$\sigma_{xx} - \mu\frac{\partial^2 \sigma_{xx}}{\partial x^2} = E\varepsilon_{xx} \tag{5}$$

where σ and ε are the nonlocal stress and strain respectively, $\mu = (e_0 a)^2$ is nonlocal parameter, E is the elasticity modulus.

2.2 The Euler-Bernoulli beam theory

EBT assumes that the straight lines will remain straight and vertical to the mid-plane after deformation and this is based on the following displacement field (Reddy 2007)

$$u_1 = u(x,t) - z\frac{\partial w}{\partial x} \quad , \quad u_2 = 0 \quad , \quad u_3 = w(x,t) \tag{6}$$

where (u, w) are the axial and transverse displacements of the point on the mid-plane of the beam. The axial strain ε_{xx} of EBT is obtained as

$$\varepsilon_{xx}=\frac{\partial u}{\partial x}-z\frac{\partial^2 w}{\partial x^2}\quad,\quad \gamma_{xz}=\frac{\partial u_1}{\partial x}+\frac{\partial u_2}{\partial x}=0 \tag{7}$$

The governing equations of motion and the boundary conditions for EBT can be derived by Hamilton's principles as follows

$$\int_0^t \delta(T-U+V)dt=0 \tag{8}$$

where U is the strain energy, T is the kinetic energy and V is the work done by external forces. The first variation of the strain energy can be calculated as

$$\delta\, U=\int_v \sigma_{ij}\delta\varepsilon_{ij}dV=\int_v(\sigma_{xx}\delta\varepsilon_{xx})dV \tag{9}$$

Substituting Eq. (7) into Eq. (9) yields

$$\delta\, U=\int_0^L\left[N\delta\left(\frac{\partial u}{\partial x}\right)-M\delta\left(\frac{\partial^2 w}{\partial x^2}\right)\right]dx \tag{10}$$

where N , M are the axial force and bending moment, respectively. The stress resultants used in Eq. (10) are defined as

$$N=\int_A \sigma_{xx}dA\quad,\quad M=\int_A \sigma_{xx}zdA \tag{11}$$

And the kinetic energy for Euler-Bernoulli beam can be written as

$$T=\frac{1}{2}\int_0^L\int_A \rho\left((\frac{\partial u_1}{\partial t})^2+(\frac{\partial u_3}{\partial t})^2\right)dAdx \tag{12}$$

The first variation of the Eq. (12) can be obtained as

$$\delta\, T=\int_0^L\left[\rho A\frac{\partial u}{\partial t}\delta(\frac{\partial u}{\partial t})+\rho A\frac{\partial w}{\partial t}\delta(\frac{\partial w}{\partial t}))+\rho I\frac{\partial^2 w}{\partial t\partial x}\delta(\frac{\partial^2 w}{\partial t\partial x})\right]dx \tag{13}$$

where ρ, I ,A are the mass density, rotational inertia and cross-sectional area of the nanobeams, respectively. The first variation of the work of external forces can be written in the following form

$$\delta\, V=\int_0^L\left(f\delta u+q\delta w\right)dx \tag{14}$$

In which f and q are external axial and transverse load distribution along the length of beam, respectively. Substituting Eqs. (10), (13) and (14) into Eq. (8) and setting the coefficients of δu, δw and $\delta(\frac{\partial w}{\partial x})$ to zero, leads to the following motion equations

$$\frac{\partial N}{\partial x} + f = \rho A \frac{\partial^2 u}{\partial t^2} \tag{15a}$$

$$\frac{\partial^2 M}{\partial x^2} - \frac{\partial}{\partial x}\left(\bar{N}\frac{\partial w}{\partial x}\right) + q = \rho A \frac{\partial^2 w}{\partial t^2} - \rho I \frac{\partial^4 w}{\partial t^2 \partial x^2} \tag{15b}$$

Integrating Eq. (5) over the beam's cross-section area, the force-strain and the moment-strain of the nonlocal EBT can be obtained as follows

$$N - \mu \frac{\partial^2 N}{\partial x^2} = EA \frac{\partial u}{\partial x} \tag{16a}$$

$$M - \mu \frac{\partial^2 M}{\partial x^2} = -EI \frac{\partial^2 w}{\partial x^2} \tag{16b}$$

The explicit relation of the nonlocal normal force and bending moment can be derived by substituting the second derivative of M from Eq. (15) into Eq. (16) as follows

$$N = EA \frac{\partial u}{\partial x} + \mu \left(\frac{\partial^3 u}{\partial x \partial t^2} - \frac{\partial f}{\partial x} \right) \tag{17a}$$

$$M = -EI \frac{\partial^2 w}{\partial x^2} + \mu \left(\frac{\partial}{\partial x}\left(\bar{N}\frac{\partial w}{\partial x}\right) - q + \rho A \frac{\partial^2 w}{\partial t^2} - \rho I \frac{\partial^4 w}{\partial t^2 \partial x^2} \right) \tag{17b}$$

The nonlocal governing equations of Euler-Bernoulli nanobeams in terms of displacements can be derived by substituting N and M from Eq. (17) into Eq. (15) as follows

$$\frac{\partial}{\partial x}\left(EA\frac{\partial u}{\partial x}\right) + f - \mu \frac{\partial^2 f}{\partial x^2} = \rho A \frac{\partial^2 u}{\partial t^2} - \mu \rho A \frac{\partial^4 u}{\partial t^2 \partial x^2} \tag{18a}$$

$$\begin{aligned} &\frac{\partial^2}{\partial x^2}\left(-EI\frac{\partial^2 w}{\partial x^2}\right) + \mu \frac{\partial^2}{\partial x^2}\left[\frac{\partial}{\partial x}\left(\bar{N}\frac{\partial w}{\partial x}\right) - q + \rho A \frac{\partial^2 w}{\partial t^2} - \rho I \frac{\partial^4 w}{\partial t^2 \partial x^2}\right] + q \\ &- \frac{\partial}{\partial x}\left(\bar{N}\frac{\partial w}{\partial x}\right) = \rho A \frac{\partial^2 w}{\partial t^2} - \rho I \frac{\partial^4 w}{\partial t^2 \partial x^2} \end{aligned} \tag{18b}$$

3. Problem statement

3.1 Brief statement of problem

A nanobeam with simply-supported boundary condition is presented in Fig. 1. As described in previous section, the governing equation for vibration of an Euler–Bernoulli nanobeam subjected to pre-stress load can be obtained by setting $f = 0$, $q = 0$ and neglecting the rotational inertia (ρI) in Eq. (18(b)) as follows

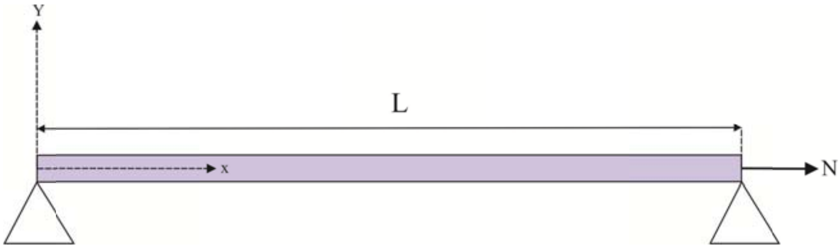

Fig. 1 Ssimply-supported nanobeam at both ends

$$\frac{\partial^2}{\partial x^2}\left(EI\frac{\partial^2 w}{\partial x^2}\right)+\rho A\frac{\partial^2 w}{\partial t^2}-\mu\frac{\partial^2}{\partial x^2}\left[\frac{\partial}{\partial x}\left(\bar{N}\frac{\partial w}{\partial x}\right)+\rho A\frac{\partial^2 w}{\partial t^2}\right]+\frac{\partial}{\partial x}\left(\bar{N}\frac{\partial w}{\partial x}\right)=0 \tag{19}$$

where E is the Young's modulus, I second moment of area about the y-axis, w the deflection of the beam, ρ density of the nanobeam, A cross section area of the nanobeam, L nanobeam length and $\bar{N}$ represents the axial force on the nanobeam and is expressed as

$$\bar{N}=N_m+N_\theta \tag{20}$$

In which N_m is the axial force due to the mechanical loading prior to buckling and N_θ is the axial force due to the influence of temperature changes. Based on the theory of thermal elasticity mechanics, the thermal axial force N_θ can be written as (Zhang *et al*. 2008)

$$N_\theta=-\frac{E\,A}{1-2\nu}\alpha_x\,\theta \tag{21}$$

where α_x is the coefficient of thermal expansion in the direction of X-axis, ν is the Poisson's ratio and θ denotes the changes in temperature. Here the following B.C.s are considered (Pradhan and Reddy 2011)

$$w(0,t)=\varepsilon a_1(t);\ \frac{\partial^2 w(0,t)}{\partial^2 x}=\varepsilon b_1(t);\ w(1,t)=\varepsilon a_2(t);\ \frac{\partial^2 w(1,t)}{\partial^2 x}-R_4\,L^2 w(l,t)=\varepsilon b_2(t) \tag{22a}$$

where

$$R_4=\frac{\mu\,k_w}{(E\,I-\mu P_{res})} \tag{22b}$$

in which k_w is the Winkler constant and P_{res} denotes the axial load and ε is a small perturbation parameter. Theses B.Cs mean that the both ends of the beam are allowed to have small deflections and moments as deviations from the ideal state. In order to have the same time variations at the boundaries, the following relations are held

$$w(0,t)=\varepsilon a_1;\quad \frac{\partial^2 w(0,t)}{\partial^2 x}=\varepsilon b_1;\quad w(1,t)=\varepsilon a_2;\quad \frac{\partial^2 w(1,t)}{\partial^2 x}-R_4\,L^2 w(\boldsymbol{l},t)=\varepsilon b_2 \tag{23}$$

where a_1, a_2, b_1, b_2 are constant amplitudes with the following values:

- $a_1 = a_2 = 1, b_1 = b_2 = 0$:for non-ideal B.Cs at one end,
- $a_1 = a_2 = b_1 = b_2 = 1$: for non-ideal B.Cs at the both ends

3.1 Solution procedure

The solution of the Eq. (19) is considered as

$$W(x,t) = (A\cos\omega t + B\sin\omega t)\ Y(x) \tag{24}$$

By substituting the above relation into Eq. (19) and the B.Cs (23), one may obtain

$$(EI - \mu^2 \bar{N})Y^{(4)} + (\bar{N} + \mu^2 \rho A\omega^2)Y'' - \rho A\omega^2 Y = 0 \tag{25a}$$

$$Y(0) = \varepsilon a_1,\quad Y''(0) = \varepsilon b_1,\quad Y(1) = \varepsilon a_2,\quad Y''(1) = \varepsilon b_2 \tag{25b}$$

Using Lindstedt-Poincare technique, the frequencies and mode shapes in the perturbation series are expanded as

$$Y = Y_0 + \varepsilon Y_1 + \ldots, \qquad \omega = \omega_0 + \varepsilon\,\omega_1 + \ldots \tag{26}$$

Now substituting the above relations into Eq. (25) and separating the coefficients with the same order gives

$$O(1):\quad \begin{cases} (EI - \mu^2 \bar{N})Y_0^{(4)} + (\bar{N} + \mu^2 \rho A\omega_0^{\ 2})\ Y_0'' - \rho A\omega^2 Y_0 = 0\,; \\ Y_0(0) = Y_0''(0) = Y_0(1) = Y_0''(1) = 0 \end{cases} \tag{27}$$

$$O(\varepsilon):\quad \begin{cases} (EI - \mu^2 \bar{N})Y_1^{(4)} + (\bar{N} + \mu^2 \rho A\omega_0^{\ 2})\ Y_1'' - \rho A\omega_0^{\ 2} Y_1 = 2\,\omega_0\,\omega_1\,(\rho A Y_0 - \mu^2 \rho A Y_0'') \\ Y_1(0) = a_1,\quad Y_1''(0) = b_1, Y_1(1) = a_2, Y_1''(1) = b_2\,; \end{cases} \tag{28}$$

Considering a solution with the form of $Y_0(x) = e^{kx}$ and substituting it into Eq. (27) yields to the following characteristic equation:

$$(EI - \mu^2 \bar{N})k^4 + (\bar{N} + \mu^2 \rho A\omega_0^{\ 2})k^2 - \rho A\omega_0^{\ 2} = 0 \tag{29}$$

while the roots characteristic Eq. (29) can be obtained as

$$k^2 = \frac{-(\bar{N} + \mu^2 \rho A\omega_0^{\ 2}) \mp \sqrt{(\bar{N} + \mu^2 \rho A\omega_0^{\ 2})^2 + 4(EI - \mu^2 \bar{N})\rho A\omega_0^{\ 2}}}{2(EI - \mu^2 \bar{N})} \tag{30}$$

Since: $(\bar{N} + \mu^2 \rho A\omega_0^{\ 2})^2 + 4(EI - \mu^2 \bar{N})\rho A\omega_0^{\ 2} > 0$ and : $\sqrt{(\bar{N} + \mu^2 \rho A\omega_0^{\ 2})^2 + 4(EI - \mu^2 \bar{N})\rho A\omega_0^{\ 2}} > p$, the following relations can be written

$$k_1 = \pm\left(\frac{-(\bar{N}+\mu^2\rho A\omega_0^{\,2})+\sqrt{(\bar{N}+\mu^2\rho A\omega_0^{\,2})^2+4(EI-\mu^2\bar{N})\rho A\omega_0^{\,2}}}{2(EI-\mu^2\bar{N})}\right)^{\frac{1}{2}} = \pm s_1 \quad ,$$
$$k_2 = \pm i\left(\frac{-(\bar{N}+\mu^2\rho A\omega_0^{\,2})\mp\sqrt{(\bar{N}+\mu^2\rho A\omega_0^{\,2})^2+4(EI-\mu^2\bar{N})\rho A\omega_0^{\,2}}}{2(EI-\mu^2\bar{N})}\right)^{\frac{1}{2}} = \pm i\,s_2 \tag{31}$$

In view of the above relations, the solution of the Eq. (27) can be written as

$$Y_0(x) = A\cosh\ s_1 x + B\sinh s_1 x + C\sin s_2 x + D\cos s_2 x \tag{32}$$

Prescribing the B.Cs given in relation (27), the coefficients of the Eq. (32) are obtained as

$$\left.\begin{aligned} Y_0(0)&=0\\ Y_0''(0)&=0\end{aligned}\right\}\Rightarrow\quad A=D=0$$
$$\left.\begin{aligned} Y_0(1)&=0\\ Y_0''(1)&=0\end{aligned}\right\}\quad 2\sinh s_1\ \sin s_2 = 0 \tag{33}$$

In above relation, as $\sinh\ s_1 \neq 0$, so $B=0$ and the following expression is obtained

$$\sin s_2 = 0 \quad\Rightarrow\quad \sin s_2 = \sin n\pi \quad\Rightarrow\quad s_2 = n\pi \tag{34}$$

Considering the above relation, ω_0 can be written as

$$\left(\frac{-(\bar{N}+\mu^2\rho A\omega_0^{\,2})\mp\sqrt{(\bar{N}+\mu^2\rho A\omega_0^{\,2})^2+4(EI-\mu^2\bar{N})\rho A\omega_0^{\,2}}}{2(EI-\mu^2\bar{N})}\right)^{\frac{1}{2}} = (n\pi)^2$$
$$\Rightarrow\quad \omega_0 = \pi\sqrt{\frac{L^2n^2N+n^4\pi^2(EI-N\mu^2)}{AL^2\rho(L^2+n^2\pi^2\mu^2)}} \tag{35}$$

Now with the determined coefficients, the solution of the Eq. (27) can be written as

$$Y_0(x) = C\sin s_2 x \tag{36}$$

Normalizing $Y_0(x)$ by relation $\int_0^1 Y_0^{\,2}\,dx = 1$, one may obtain: $C=\sqrt{2}$ So

$$Y_0(x) = \sqrt{2}\ \sin s_2 x \tag{37}$$

The solution of the Eq. (28), noting the relevant B.C.'s, is considered as

$$Y_1(x) = Y_{1h}(x) + Y_{1p}(x) \tag{38}$$

where $Y_{1h}\left(x\right)$ and $Y_{1p}\left(x\right)$ are the homogenous and the particular solutions of the Eq. (28) respectively, which are as follows

$$Y_{1h}\left(x\right)=A\sinh s_1 x+B\cosh s_1 x+C\sin s_2 x+D\cos s_2 x \tag{39}$$

$$Y_{1p}\left(x\right)=x\left(N_1\sin s_2 x+N_2\cos s_2 x\right) \tag{40}$$

Inserting $Y_{1p}\left(x\right)$ in Eq. (28), in order to obtain the constants N_1, N_2, the following relation is obtained:

$$\begin{aligned}&4(EI-\mu^2\bar{N})s_2^{\,3}\left(-N_1\cos s_2 x+N_2\sin s_2 x\right)+(EI-\mu^2\bar{N})x\left(N_1 s_2^{\,4}\sin s_2 x+N_2 s_2^{\,4}\cos s_2 x\right)\\&+(\bar{N}+\mu^2\rho A\omega_0^{\,2})\left[2s_2\left(N_1\cos s_2 x-N_2\sin s_2 x\right)-s_2^{\,2}x\left(-N_1\sin s_2 x-N_2\cos s_2 x\right)\right]\\&-\rho A\omega_0^{\,2}x\left(N_1\sin s_2 x+N_2\cos s_2 x\right)=2\sqrt{2}\,\omega_0\,\omega_1(1+s_2^{\,2})\sin s_2 x\end{aligned} \tag{41}$$

It can be shown that the sum of the coefficients of the expression $x\left(N_1\sin s_2 x+N_2\cos s_2 x\right)$ related to the second, fourth and fifth terms of the left hand side of the above equation equals to zero, so, rewriting Eq. (41) in view of the above relations, one may obtain

$$\begin{aligned}&4(EI-\mu^2\bar{N})s_2^{\,3}\left(-N_1\cos s_2 x+N_2\sin s_2 x\right)+(\bar{N}+\mu^2\rho A\omega_0^{\,2})\\&*\left[2s_2\left(N_1\cos s_2 x-N_2\sin s_2 x\right)\right]=2\sqrt{2}\,\omega_0\,\omega_1(1+s_2^{\,2})\sin s_2 x\end{aligned} \tag{42}$$

Equating the coefficients of the terms $\sin s_2 x$ and $\cos s_2 x$ of the both sides of Eq. (41) to obtain constants N_1 and N_2 may be resulted in the following

$$\begin{aligned}&-2N_1 s_2\left(2(EI-\mu^2\bar{N})s_2^{\,2}-(\bar{N}+\mu^2\rho A\omega_0^{\,2})\right)=0\\&4(EI-\mu^2\bar{N})N_2 s_2^{\,3}-2(\bar{N}+\mu^2\rho A\omega_0^{\,2})N_2 s_2=2\sqrt{2}(1+s_2^{\,2})\omega_0\,\omega_1\end{aligned} \tag{43}$$

Since $2(EI-\mu^2\bar{N})\,s_2^{\,2}-(\bar{N}+\mu^2\rho A\omega_0^{\,2})\neq 0$, from the first equation of Eq. (43), it is obtained that $N_1=0$ and from the second equation of Eq. (43), N_2 is obtained as

$$N_2=\frac{\sqrt{2}\omega_0\,\omega_1(1+s_2^2)}{2(EI-\mu^2\bar{N})s_2^{\,3}-(\bar{N}+\mu^2\rho A\omega_0^{\,2})s_2} \tag{44}$$

Substituting the coefficients N_1 and N_2 in Eq. (40), the particular solution of Eq. (26) is obtained as

$$Y_{1p}\left(x\right)=\frac{\sqrt{2}\omega_0\,\omega_1(1+s_2^2)}{2(EI-\mu^2\bar{N})s_2^{\,3}-(\bar{N}+\mu^2\rho A\omega_0^{\,2})s_2}x\cos s_2 x \tag{45}$$

Hence the sum of the particular and the homogenous solutions of the differential Eq. (28), can be written as

$$Y_1(x) = A\sinh s_1 x + B\cosh s_1 x + C\sin s_2 x + D\cos s_2 x + \frac{\sqrt{2}\omega_0\,\omega_1(1+s_2^2)}{2(EI-\mu^2\,\bar{N})s_2^{\,3} - (\bar{N}+\mu^2\,\rho A\omega_0^{\,2})\,s_2}\, x\cos s_2\, x \tag{46}$$

Prescribing the B.C.'s related to the Eq. (28), the constants of the above relation are obtained as

$$\begin{aligned} &Y_1(0) = B + D = a_1 \\ &Y_1''(0) = Bs_1^{\,2} - Ds_2^{\,2} = b_1 \\ &Y_1(1) = A\sinh s_1 + B\cosh s_1 + C\sin s_2 + D\cos s_2 + N_2\,\cos s_2 = a_2 \\ &Y_1''(1) = As_1^{\,2}\sinh s_1 + Bs_1^{\,2}\cosh s_1 - Cs_2^{\,2}\sin s_2 - Ds_2^{\,2}\cos s_2 - N_2\left(2s_1^{\,2}\cos s_1 + s_2^{\,2}\cos s_2\right) = b_2 \end{aligned} \tag{47}$$

According to Eq. (34), the term $\sin s_2$ is equal to zero. By setting $\sin s_2 = 0$ in above relations, it is seen that the coefficient C vanishes, so it is assumed that the coefficient C is zero. From the two first Eq. (47) it is obtained that

$$\begin{aligned} B &= a_1 - \frac{a_1 s_1^{\,2} - b_1}{s_1^{\,2} + s_2^{\,2}} \\ D &= \frac{a_1 s_1^{\,2} - b_1}{s_1^{\,2} + s_2^{\,2}} \end{aligned} \tag{48}$$

Multiplying the third part of the Eq. (47) by $-s_1^2$ and adding the resulted equation to the forth equation, produces the following characteristic equation from which ω_1 can be obtained

$$\left(b_1 - a_1 s_1^{\,2}\right)\cos s_2 - \frac{\sqrt{2}\omega_0\,\omega_1(1+s_2^2)}{2(EI-\mu^2\,\bar{N})s_2^{\,3} - (\bar{N}+\mu^2\,\rho A\omega_0^{\,2})\,s_2}\left(s_1^{\,2}+s_2^{\,2}\right)\cos s_2 = b_2 - a_2 s_1^{\,2} \tag{49}$$

ω_1 is obtained from the above equation as following

$$\omega_1 = \frac{\left(2(EI-\mu^2\,\bar{N})s_2^{\,3} - (\bar{N}+\mu^2\,\rho A\omega_0^{\,2})\,s_2\right)\left[\left(b_1 - a_1 s_1^{\,2}\right)\cos s_2 + a_2 s_1^{\,2} - b_2\right]}{\sqrt{2}\omega_0\left(1+s_2^2\right)\left(s_1^{\,2}+s_2^{\,2}\right)\cos s_2} \tag{50}$$

If the third part of Eq. (47) is multiplied by s_2^2 and added to the forth equation, the following equation will be obtained

$$A\left(s_1^{\,2}+s_2^{\,2}\right)\sinh s_1 + B\left(s_1^{\,2}+s_2^{\,2}\right)\cosh s_1 - \frac{\sqrt{2}\omega_0\,\omega_1(1+s_2^2)}{2(EI-\mu^2\,\bar{N})s_2^{\,3} - (\bar{N}+\mu^2\,\rho A\omega_0^{\,2})\,s_2}\,2s_1^{\,2}\,s_2^{\,2}\cos s_1 = a_2 s_2^{\,2} + b_2 \tag{51}$$

Substituting the constant B from Eq. (48) into the above equation yields the constant A as

$$A=\frac{\left[\left(a_2 s_2^{\,2}+b_2\right)-\left(a_1-\frac{a_1 s_1^{\,2}-b_1}{s_1^{\,2}+s_2^{\,2}}\right)\left(s_1^{\,2}+s_2^{\,2}\right)\cosh s_1+\frac{\sqrt{2}\omega_0\,\omega_1(1+s_2^2)}{2(EI-\mu^2\,\bar{N})s_2^{\,3}-(\bar{N}+\mu^2\,\rho A\omega_0^{\,2})s_2}\,2s_1^{\,2}\,s_2^{\,2}\cos s_1\right]}{\left(s_1^{\,2}+s_2^{\,2}\right)\sinh s_1} \tag{52}$$

Now substituting the constants A, B and D into the Eq. (46), $Y_1(x)$ is obtained as follows

$$Y_1(x)=\frac{\left[\left(a_2 s_2^{\,2}+b_2\right)-\left(a_1-\frac{a_1 s_1^{\,2}-b_1}{s_1^{\,2}+s_2^{\,2}}\right)\left(s_1^{\,2}+s_2^{\,2}\right)\cosh s_1+\frac{\sqrt{2}\omega_0\,\omega_1(1+s_2^2)}{2(EI-\mu^2\,\bar{N})s_2^{\,3}-(\bar{N}+\mu^2\,\rho A\omega_0^{\,2})s_2}\,2s_1^{\,2}\,s_2^{\,2}\cos s_1\right]}{\left(s_1^{\,2}+s_2^{\,2}\right)\sinh s_1}. \tag{53}$$
$$\sinh s_1 x+\left(a_1-\frac{a_1 s_1^{\,2}-b_1}{s_1^{\,2}+s_2^{\,2}}\right)\cosh s_1 x+\left(\frac{a_1 s_1^{\,2}-b_1}{s_1^{\,2}+s_2^{\,2}}\right)\cos s_2 x+\frac{\sqrt{2}\omega_0\,\omega_1(1+s_2^2)}{2(EI-\mu^2\,\bar{N})s_2^{\,3}-(\bar{N}+\mu^2\,\rho A\omega_0^{\,2})s_2}\,x\cos s_2 x$$

Having $Y_0(x)$ and $Y_1(x)$ from Eqs. (37) and (44) respectively, the solution of the differential Eq. (19) is obtained as following

$$Y=\sqrt{2}\,\sin s_2 x+\varepsilon\left\{\frac{\left[\left(a_2 s_2^{\,2}+b_2\right)-\left(a_1-\frac{a_1 s_1^{\,2}-b_1}{s_1^{\,2}+s_2^{\,2}}\right)\left(s_1^{\,2}+s_2^{\,2}\right)\cosh s_1+\frac{\sqrt{2}\omega_0\,\omega_1(1+s_2^2)}{2(EI-\mu^2\,\bar{N})s_2^{\,3}-(\bar{N}+\mu^2\,\rho A\omega_0^{\,2})s_2}\,2s_1^{\,2}\,s_2^{\,2}\cos s_1\right]}{\left(s_1^{\,2}+s_2^{\,2}\right)\sinh s_1}.\right. \tag{54}$$
$$\left.\sinh s_1 x+\left(a_1-\frac{a_1 s_1^{\,2}-b_1}{s_1^{\,2}+s_2^{\,2}}\right)\cosh s_1 x+\left(\frac{a_1 s_1^{\,2}-b_1}{s_1^{\,2}+s_2^{\,2}}\right)\cos s_2 x+\frac{\sqrt{2}\omega_0\,\omega_1(1+s_2^2)}{2(EI-\mu^2\,\bar{N})s_2^{\,3}-(\bar{N}+\mu^2\,\rho A\omega_0^{\,2})s_2}\,x\cos s_2 x\right\}$$

Moreover, from Eqs. (35) and (50), the parameter ω appeared in Eq. (19) is derived as following

$$\omega=\pi\sqrt{\frac{L^2n^2N+n^4\pi^2(EI-N\mu^2)}{AL^2\rho(L^2+n^2\pi^2\mu^2)}}+\varepsilon\left[\frac{\left(2(EI-\mu^2\,\bar{N})s_2^{\,3}-(\bar{N}+\mu^2\,\rho A\omega_0^{\,2})s_2\right)\left[\left(b_1-a_1 s_1^{\,2}\right)\cos s_2+a_2 s_1^{\,2}-b_2\right]}{\sqrt{2}\omega_0\left(1+s_2^2\right)\left(s_1^{\,2}+s_2^{\,2}\right)\cos s_2}\right] \tag{55}$$

Now using Eqs. (54) and (55) , the mode shapes and the frequencies of the nanobeam subjected to axial loading with non-ideal B.C.'s can be obtained respectively.

4. Validation of the analysis

In this section, the accuracy and the efficiency of the presented method and closed form solutions are investigated through some examples. For this purpose, nanobeams with the following properties are assumed in computing the numerical values (Reddy 2007)

$$L=10,\ \ \nu=0.3,\ \ \rho=1,\ \ I=bh^3/12,\ \ E=30*10^6,\ \ \alpha_x=-1.6*10^6$$

Firstly, the accuracy of the nonlocal natural frequencies of nanobeam is investigated. Table 1 presents the non-dimensional fundamental frequencies of nonlocal nanobeams $\hat{\omega}=\omega L^2\sqrt{\rho A/EI}$

with ideal B.Cs compared to the results given by Reddy (2007), Thai (2012) which shows a good agreement. It can be observed that increasing the nonlocality parameter tends to decrease in natural frequency of the nanobeams due to the decrease in the stiffness of the nanostructure.

Next, the first normalized natural frequencies of a nanobeam with different aspect ratio and various nonlocal parameters μ are presented in Tables 2 for ideal B.Cs and non-ideal B.Cs at one end and both ends. The nonlocal parameters are taken as 0, 1, 2, 3, and 4 nm^2.

It should be noted that μ=0 corresponds to the local beam theory. Also, note that $\varepsilon = 0$ corresponds to the frequencies and mode shapes for ideal B.Cs. It can be seen that increasing the aspect ratio tends to increase the natural frequency while increasing nonlocal parameter tends to decrease the natural frequency.

Fig. 2 shows the effect of preload parameter on fundamental frequency of a nanobeam with non-ideal B.Cs at both ends with different perturbation parameters and aspect ratios. It is seen that the fundamental frequency increases by increasing the axial load from compressive to tensile values.

Table 1 Comparison of non-dimensional fundamental natural frequencies for simply supported nanobeams

L/h	μ	Analytical (Thai 2012)	Analytical (Reddy 2007)	Perturbation method (Present study)
10	0	9.8293	9.8696	9.86960440
	1	9.3774	9.4159	9.41588108
	2	8.9826	9.0195	9.01948110
	3	8.6338	8.6693	8.66926898
	4	8.3228	8.3569	8.35691990
20	0	9.8595	9.8696	9.86960440
	1	9.4062	9.4159	9.41588108
	2	9.0102	9.0195	9.01948110
	3	8.6604	8.6693	8.66926898
	4	8.3483	8.3569	8.35691990
100	0	9.8692	9.8696	9.86960440
	1	9.4155	9.4159	9.41588108
	2	9.0191	9.0195	9.01948110
	3	8.6689	8.6693	8.66926898
	4	8.3566	8.3569	8.35691990

Table 2 Comparison of the first non-dimensional natural frequencies for the ideal ($\varepsilon = 0$) and non-ideal ($\varepsilon = 0.1$) B.Cs when N=0, $\theta = 0$

L/h	μ	ω (ideal) (Reddy 2007)	ω (NIOE*)	ω (NIBE**)
10	0	9.8696	9.6825	9.4753
	1	9.4158	9.2204	9.0021
	2	9.0194	8.8181	8.1688
	3	8.6692	8.4641	9.0094
	4	8.3569	8.1496	8.3942
20	0	9.8696	9.8228	9.7710
	1	9.4158	9.3670	9.3124
	2	9.0194	8.9691	8.8068
	3	8.6692	8.6179	8.7543
	4	8.3569	8.3050	8.3662
100	0	9.8696	9.8677	9.8656
	1	9.4158	9.4139	9.4117
	2	9.0194	9.0174	9.0109
	3	8.6692	8.6672	8.6726
	4	8.3569	8.3548	8.3572

* NIOE: non-ideal B.C at one end

** NIBE: non-ideal B.C at both end

The other noticeable point is that by increasing the perturbation parameter at a specific axial load, the fundamental frequency decreases. On the other hand, increasing aspect ratio tends to make a convergence of all three conditions to the state of ideal B.Cs. The reason is that by increasing aspect ratio, the beam becomes thicker and stiffer while the non-ideal B.Cs tends to decrease the stiffness of the nanostructures and hence decreases the values of natural frequencies.

Table 3 illustrates the variations of the fundamental frequency with respect to the perturbation parameter for L/h=100, N=0 and $\theta = 0$ while nonlocal parameters are taken as 0, 1 and 2 nm^2. It is observed that the fundamental frequency of the nanobeams decreases by increasing the perturbation parameter for different values of nonlocal parameters. Also, Fig. 3 shows the variations of the fundamental frequency with respect to the perturbation parameter for aspect ratios equal to 20 and 50.

The fundamental frequency parameter as a function of temperature change is presented in Table 4 for a nanobeam with different nonlocal parameters. Also, Table 5 and Fig. 3 present the variations of the first dimensionless natural frequency of the nanobeam with respect to temperature change for different values of aspect ratios and nonlocal parameters. Observing these figures, it is easily deduced that, an increase in nonlocal parameter leads to a decrease in the first dimensionless natural frequency for all temperature changes and aspect ratios. In addition, it is deduced that the fundamental frequency may increase by increasing the temperature changes and thus the temperature change has a significant effect on the fundamental frequency of the nanobeams which cannot be ignored.

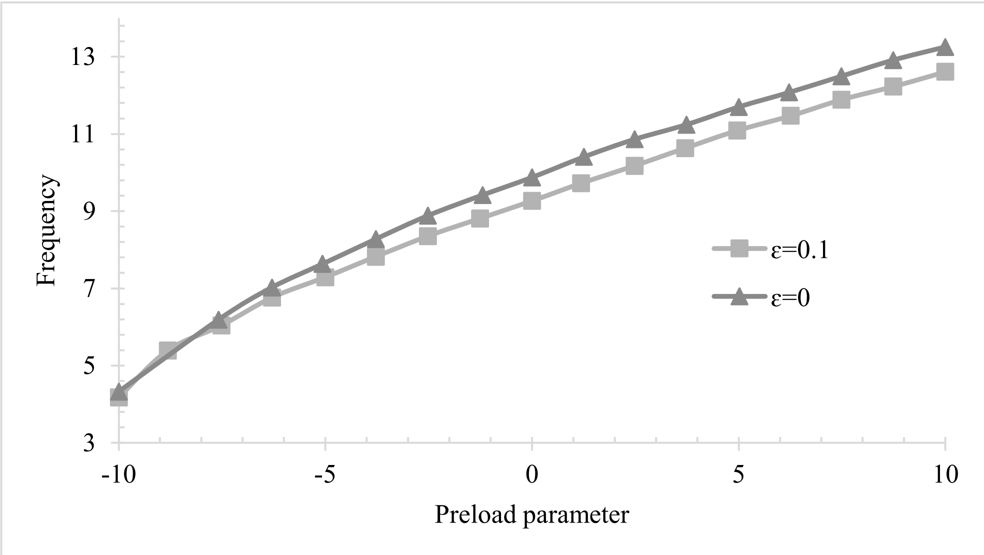

L/h=20

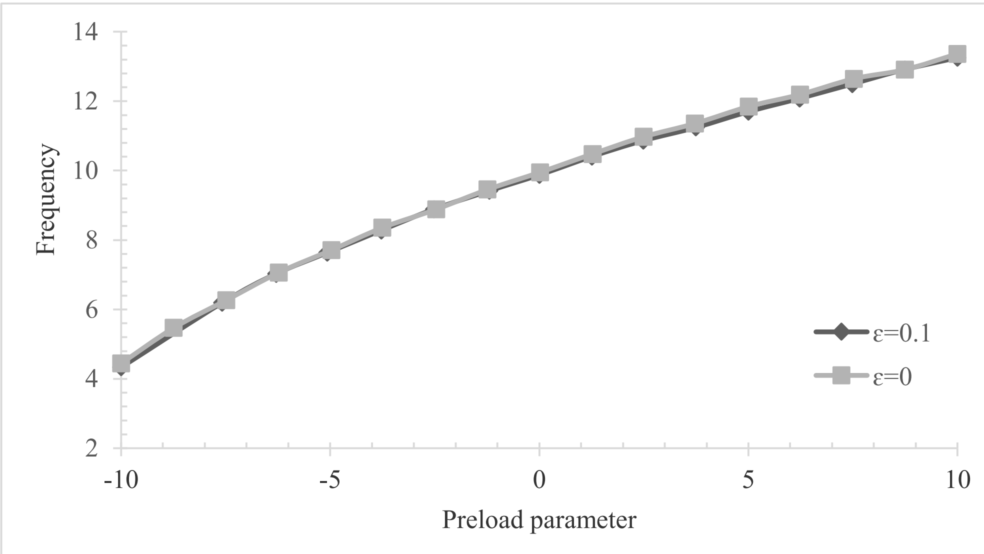

L/h=50

Fig. 2 Fundamental frequency versus preload parameter for different perturbation parameters and aspect ratios with non-ideal B.Cs at both ends and $\mu = 0,\ \theta = 0$, L/h=20

Table 3 Comparison between the first non-dimensional natural frequencies of the nanobeams with ideal and non-ideal B.Cs with different perturbation parameters (N=0, L/h=100, $\theta = 0$)

ε	$\mu = 0\ nm^2$			$\mu = 1\ nm^2$			$\mu = 2\ nm^2$		
	ω (ideal)	ω (NIOE*)	ω (NIBE**)	ω (ideal)	ω (NIOE*)	ω (NIBE**)	ω (ideal)	ω (NIOE*)	ω (NIBE**)
0	9.8696	9.8696	9.8696	9.4158	9.4158	9.4158	9.0194	9.0194	9.0194
0.1	9.8696	9.8636	9.8571	9.4158	9.4097	9.4028	9.0194	9.0131	8.9925
0.2	9.8696	9.8577	9.8446	9.4158	9.4035	9.3897	9.0194	9.0067	8.9656
0.3	9.8696	9.8518	9.8322	9.4158	9.3973	9.3766	9.0194	9.0003	8.9387
0.4	9.8696	9.8459	9.8197	9.4158	9.3911	9.3635	9.0194	8.9940	8.9118
0.5	9.8696	9.8400	9.8072	9.4158	9.3849	9.3504	9.0194	8.9876	8.8849
0.6	9.8696	9.8341	9.7948	9.4158	9.3788	9.3373	9.0194	8.9812	8.8580
0.7	9.8696	9.8282	9.7823	9.4158	9.3726	9.3242	9.0194	8.9749	8.8311
0.8	9.8696	9.8222	9.7698	9.4158	9.3664	9.3112	9.0194	8.9685	8.8042
0.9	9.8696	9.8163	9.7574	9.4158	9.3602	9.2981	9.0194	8.9621	8.7773
1.0	9.8696	9.8104	9.7449	9.4158	9.3540	9.2850	9.0194	8.9558	8.7504

* NIOE: non-ideal B.C at one end ** NIBE: non-ideal B.C at both ends

Table 4a Effect of temperature on first natural frequencies with different aspect ratios (N=0, $\mu = 1\ nm^2$)

L/h	$\theta = 0$			$\theta = 20$			$\theta = 50$		
	ω (ideal)	ω (NIOE*)	ω (NIBE**)	ω (ideal)	ω (NIOE*)	ω (NIBE**)	ω (ideal)	ω (NIOE*)	ω (NIBE**)
10	9.4158	8.7979	8.1073	9.4359	8.8172	8.1319	9.4660	8.8462	8.1681
20	9.4158	9.2613	9.0887	9.4960	9.3408	9.1729	9.6150	9.4586	9.2958
30	9.4158	9.3472	9.2704	9.5953	9.5258	9.4532	9.8583	9.7878	9.7172
40	9.4158	9.3772	9.3341	9.7325	9.6932	9.6532	10.1891	10.1488	10.1073
50	9.4158	9.3911	9.3635	9.9062	9.8808	9.8553	10.5993	10.5729	10.5410
60	9.4158	9.3987	9.3795	10.1145	10.0966	10.0785	11.0801	11.0613	11.0252
70	9.4158	9.4032	9.3891	10.3552	10.3419	10.3275	11.6226	11.6085	11.4004
80	9.4158	9.4062	9.3954	10.6261	10.6158	10.6031	12.2187	12.2076	12.2330
90	9.4158	9.4082	9.3997	10.9251	10.9168	10.9037	12.8610	12.8520	12.8626
100	9.4158	9.4097	9.4028	11.2498	11.2430	11.2253	13.5428	13.5353	13.5428

* NIOE: non-ideal B.C at one end ** NIBE: non-ideal B.C at both end

Table 4b Effect of temperature on first natural frequencies with different aspect ratios (N=0, $\mu = 3\ nm^2$)

L/h	$\theta = 0$ ω (ideal)	ω (NIOE*)	ω (NIBE**)	$\theta = 20$ ω (ideal)	ω (NIOE*)	ω (NIBE**)	$\theta = 50$ ω (ideal)	ω (NIOE*)	ω (NIBE**)
10	8.6692	8.0205	9.7451	8.6911	8.0405	8.8391	8.72374	8.07051	9.99238
20	8.6692	8.5070	8.9382	8.7562	8.5922	9.1078	8.88516	8.71853	9.44242
30	8.6692	8.5971	8.7888	8.8638	8.7899	9.1916	9.14787	9.07139	10.6688
40	8.6692	8.6287	8.7365	9.0122	8.9699	9.2672	9.50347	9.45859	9.23011
50	8.6692	8.6433	8.7123	9.1995	9.1718	9.3297	9.942	9.91179	9.8481
60	8.6692	8.6512	8.6991	9.4233	9.4036	9.4876	10.453	10.4308	10.4007
70	8.6692	8.6560	8.6912	9.6812	9.6663	9.6185	11.0265	11.0091	10.9905
80	8.6692	8.6591	8.6860	9.9705	9.9587	9.9046	11.6531	11.6389	11.6248
90	8.6692	8.6612	8.6825	10.2886	10.2789	10.2642	12.3249	12.3129	12.2998
100	8.6692	8.6627	8.6800	10.6328	10.6246	10.6146	13.0347	13.0243	13.0093

* NIOE: non-ideal B.C at one end ** NIBE: non-ideal B.C at both end

Table 5 Effect of temperature on first natural frequencies with nonlocal parameter s (N=0, L/h=100)

θ	$\mu = 0\ nm^2$ ω (ideal)	ω (NIOE*)	ω (NIBE**)	$\mu = 1\ nm^2$ ω (ideal)	ω (NIOE*)	ω (NIBE**)	$\mu = 2\ nm^2$ ω (ideal)	ω (NIOE*)	ω (NIBE**)
0	9.8696	9.8636	9.8571	9.4158	9.4097	9.4028	9.0194	9.0131	8.9925
10	10.7870	10.7810	10.7522	10.3734	10.3669	10.3599	10.0150	10.0080	10.0002
20	11.6322	11.6263	11.6363	11.2498	11.2430	11.2253	10.9202	10.9126	10.9049
40	13.1608	13.1550	13.1620	12.8241	12.8168	12.8256	12.5359	12.5273	12.4608
50	13.8621	13.8564	13.8774	13.5428	13.5353	13.5428	13.2702	13.2611	13.2848

* NIOE: non-ideal B.C at one end ** NIBE: non-ideal B.C at both end

Also, Table 6 and Fig. 4 show the variation in frequency parameter with respect to nonlocal parameters for different modes of vibration. The preload parameter is assumed to be zero. It is observed that as the nonlocal parameter increases, the frequency decreases and the rate of drop of the frequency with nonlocal parameter is magnified for higher modes (*mode* = 3, 4, and 5).

And finally, Table 7 shows the variation of frequency parameter with respect to the preload parameter *N* for different modes of vibration. Five modes of vibration are considered. From Table 7, it is observed that the natural fundamental frequency will decrease and increase with increasing compressive and tensile preload, respectively and the trends are similar for all modes of vibration.

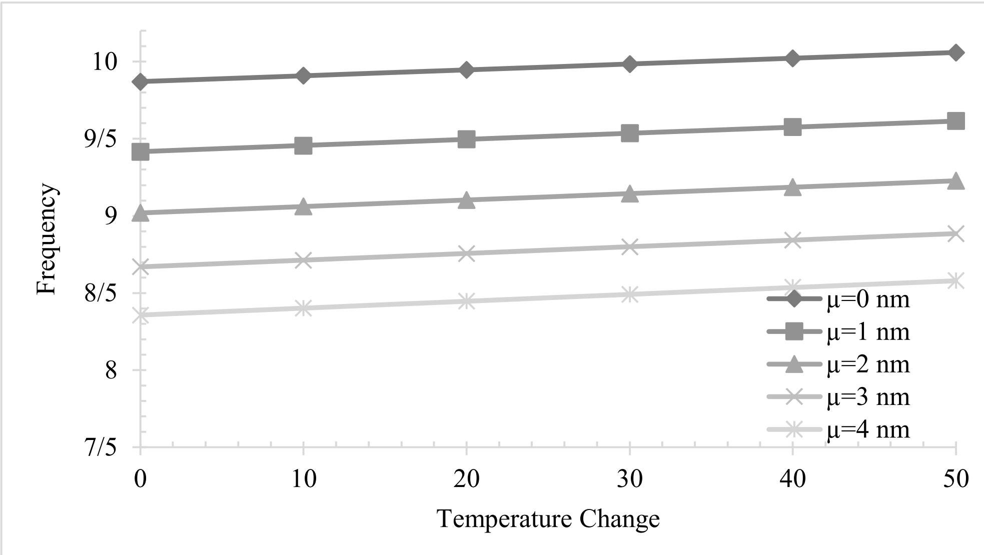

L/h=20

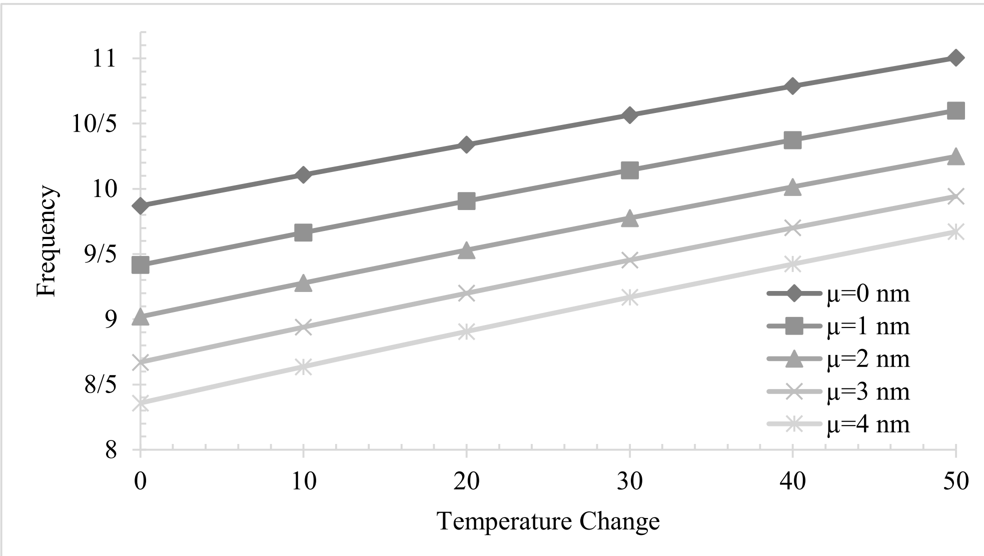

L/h=50

Fig. 3 Fundamental frequency versus the temperature change for different aspect ratio and nonlocal parameter with both side of non-ideal B.Cs and N=0

Table 6 Effect of nonlocal parameters on first three natural frequencies of nanobeams (N=0, L/h=100, θ =20)

μ	1st frequency			2nd frequency			3rd frequency		
	ω (ideal)	ω (NIOE*)	ω (NIBE**)	ω (ideal)	ω (NIOE*)	ω (NIBE**)	ω (ideal)	ω (NIOE*)	ω (NIBE**)
0	11.6322	11.6263	11.6363	41.3539	41.3478	41.3409	90.7261	90.7201	90.7136
1	11.2498	11.2430	11.2253	35.6231	35.616	35.6082	67.228	67.2216	67.2152
2	10.9202	10.9126	10.9049	31.9766	31.9696	31.9901	56.4165	56.4127	56.4062
3	10.6328	10.6246	10.6146	29.4126	29.4066	29.4157	49.9405	49.9436	49.9521
4	10.3797	10.3711	10.3115	27.4934	27.4887	28.0919	45.5415	45.5483	45.5571

Table 7 Effect of preload parameter on first three natural frequencies of nanobeam ($\mu = 2\,nm^2$, $\theta = 20$, L/h=100)

N	1st frequency			2nd frequency			3rd frequency		
	ω (ideal)	ω (NIOE*)	ω (NIBE**)	ω (ideal)	ω (NIOE*)	ω (NIBE**)	ω (ideal)	ω (NIOE*)	ω (NIBE**)
-10	4.5336	4.5331	4.5330	25.0543	25.0498	25.0651	47.9015	47.8978	47.9177
-8	6.3477	6.3470	6.3479	26.5834	26.5782	26.5847	49.7213	49.7175	49.6929
-6	7.7480	7.7450	7.7374	28.0291	28.0235	28.0292	51.4768	51.473	51.4661
-4	8.9315	8.9265	8.9209	29.4039	29.3978	29.4044	53.1744	53.1705	53.1663
-2	9.9755	9.9690	9.9625	30.7172	30.7106	30.7202	54.8194	54.8156	54.8117
0	10.920	10.9120	10.9049	31.9766	31.9696	31.9901	56.4165	56.4127	56.4062
2	11.789	11.7810	11.7721	33.1882	33.1809	32.8770	57.9696	57.9659	57.9805
4	12.598	12.5899	12.5804	34.3572	34.3495	34.3283	59.4821	59.4786	59.4823
6	13.359	13.3500	13.3405	35.4877	35.4797	35.4671	60.9572	60.9538	60.9588
8	14.0786	14.0693	14.0599	36.5832	36.575	36.5650	62.3974	62.3941	62.3879
10	14.7630	14.7537	14.7440	37.6469	37.6384	37.6294	63.8051	63.8019	63.7984

* NIOE: non-ideal B.C at one end ** NIBE: non-ideal B.C at both end

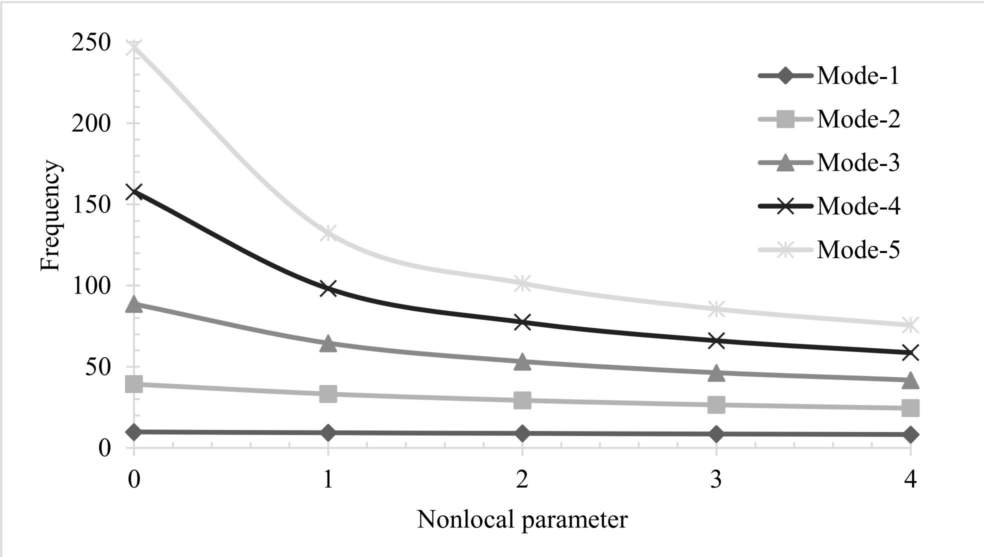

L/h=20

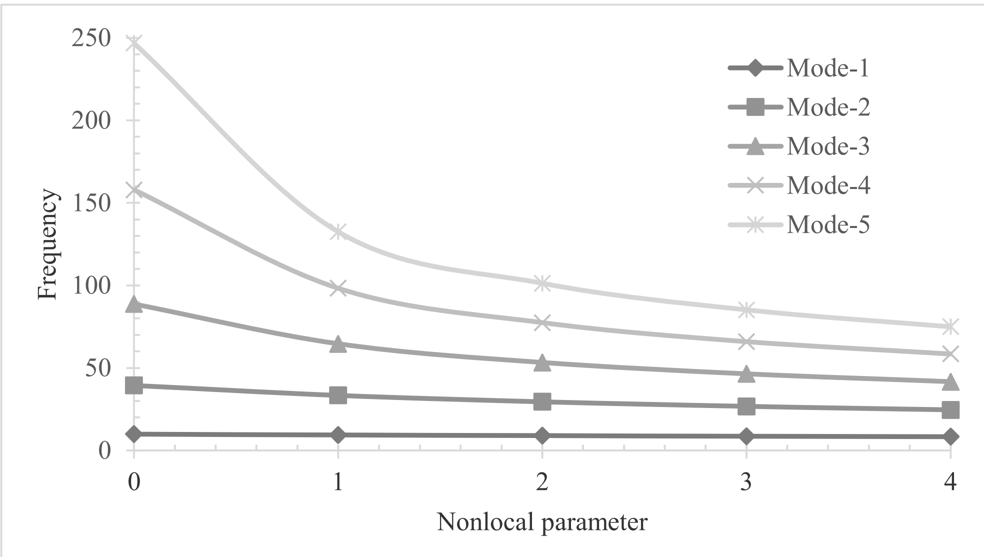

L/h=50

Fig. 4 Fundamental frequency versus nonlocal parameters for different aspect ratios and mode numbers for a nanobeam with with non-ideal B.Cs in both ends ($\mu = 0,\ \theta = 0$)

5. Conclusions

In this manuscript, the vibration analysis of a nanobeam with non-ideal boundary conditions subjected to a preload was studied based on Eringen's nonlocal elasticity theory. The governing equations are derived through Hamilton's principle while they are solved by Lindstedt - Poincare technique. The perturbation parameter is employed to model the non-ideal B.Cs and the effects of non-ideal B.Cs and preload values on the frequency of nanobeams are studied. The obtained results can be summarized as follows:

- Increasing the preload from compressive to tensile values tends to increase in fundamental frequency.
- By increasing of the perturbation parameter, the fundamental frequency of the nanobeam subjected to tensile or compressive preload decreases.
- Consideration of non-ideal B.Cs tends to decrease in natural frequencies compared to the ideal B.Cs.
- The decreasing rate of frequency respect to nonlocal parameter is magnified for higher modes of vibration.
- Fundamental frequency increases by increasing the temperature changes.

References

Ansari, R. and Sahmani, S. (2012), "Small scale effect on vibrational response of single-walled carbon nanotubes with different boundary conditions based on nonlocal beam models", *Commun. Nonlinear Sci. Numer. Simul*., **17**(4), 1965-1979.

Aydogdu, M. (2009), "A general nonlocal beam theory: its application to nanobeam bending, buckling and vibration", *Physica E: Low-dimensional Systems and Nanostructures*, **41**(9), 1651-1655.

Aydogdu, M. and Ece, M.C. (2006), "Buckling and vibration of non-ideal simply supported rectangular isotropic plates", *Mech. Res. Commun*., **33**(4), 532-540.

Belabed, Z., Houari, M.S.A., Tounsi, A., Mahmoud, S. and Bég, O.A. (2014), "An efficient and simple higher order shear and normal deformation theory for functionally graded material (FGM) plates", *Composites Part B: Engineering*, **60**, 274-283.

Bennoun, M., Houari, M.S.A. and Tounsi, A. (2016), "A novel five-variable refined plate theory for vibration analysis of functionally graded sandwich plates", *Mech. Adv. Mater. Struct*., **23**(4), 423-431.

Benzair, A., Tounsi, A., Besseghier, A., Heireche, H., Moulay, N. and Boumia, L. (2008), "The thermal effect on vibration of single-walled carbon nanotubes using nonlocal Timoshenko beam theory", *J. Phys. D: Appl. Phys*., **41**(22), 225404.

Besseghier, A., Heireche, H., Bousahla, A.A., Tounsi, A. and Benzair, A. (2015), "Nonlinear vibration properties of a zigzag single-walled carbon nanotube embedded in a polymer matrix", *Adv. Nano Res*., **3**(1), 029.

Bouderba, B., Houari, M.S.A. and Tounsi, A. (2013), "Thermomechanical bending response of FGM thick plates resting on Winkler-Pasternak elastic foundations", *Steel Compos. Struct*., **14**(1), 85-104.

Bounouara, F., Benrahou, K.H., Belkorissat, I. and Tounsi, A. (2016), "A nonlocal zeroth-order shear deformation theory for free vibration of functionally graded nanoscale plates resting on elastic foundation", *Steel Compos. Struct*., **20**(2), 227-249.

Chang, T.P. (2012), "Thermal–mechanical vibration and instability of a fluid-conveying single-walled carbon nanotube embedded in an elastic medium based on nonlocal elasticity theory", *Appl. Math. Model*., **36**(5), 1964-1973.

Civalek, Ö. and Demir, Ç. (2011a), "Bending analysis of microtubules using nonlocal Euler–Bernoulli beam

theory”, *Appl. Math.Model*., **35**(5), 2053-2067.
Civalek, Ö. and Demir, C. (2011b), “Buckling and bending analyses of cantilever carbon nanotubes using the euler-bernoulli beam theory based on non-local continuum model”, *Asian J. Civil Eng. (Building and Housing)*, **12**(5), 651-661.
Civalek, Ö., Demir, C. and Akgöz, B. (2010), “Free vibration and bending analyses of cantilever microtubules based on nonlocal continuum model”, *Math. Comput. Appl*., 15(2), 289-298.
Demir, Ç. and Civalek, Ö. (2013), “Torsional and longitudinal frequency and wave response of microtubules based on the nonlocal continuum and nonlocal discrete models”, *Appl. Math. Model*., **37**(22), 9355-9367.
Ebrahimi, F. and Salari E. (2015a), “A semi-analytical method for vibrational and buckling analysis of functionally graded nanobeams considering the physical neutral axis position”, *CMES: Computer Modeling in Engineering & Sciences* 105.2, 151-181.
Ebrahimi, F. and Salari E. (2015b), “Size-dependent free flexural vibrational behavior of functionally graded nanobeams using semi-analytical differential transform method”, *Composites Part B: Engineering*, **79**,156-169.
Eigoli, A.K. and Ahmadian, M. (2011), “Nonlinear vibration of beams under nonideal boundary conditions”, *Acta Mechanica*, **218**(3-4), 259-267.
Ekici, H.O. and Boyaci, H. (2007), “Effects of non-ideal boundary conditions on vibrations of microbeams”, *J. Vib.Control*, **13**(9-10), 1369-1378.
Eringen, A.C. (1972), “Nonlocal polar elastic continua”, *Int. J. Eng. Sci*., **10**(1), 1-16.
Eringen, A.C. (2002), *Nonlocal continuum field theories*: Springer Science & Business Media.
Eringen, A.C. and Edelen, D. (1972), “On nonlocal elasticity”, *Int. J. Eng. Sci*., **10**(3), 233-248.
Hamidi, A., Houari, M.S.A., Mahmoud, S. and Tounsi, A. (2015), “A sinusoidal plate theory with 5-unknowns and stretching effect for thermomechanical bending of functionally graded sandwich plates”, *Steel Compos. Struct*., **18**(1), 235-253.
Hebali, H., Tounsi, A., Houari, M.S.A., Bessaim, A. and Bedia, E.A.A. (2014), “New quasi-3D hyperbolic shear deformation theory for the static and free vibration analysis of functionally graded plates”, *J. Eng. Mech. - ASCE*, **140**(2), 374-383.
Mahmoud, S., Chaht, F.L., Kaci, A., Houari, M.S.A., Tounsi, A. and Bég, O.A. (2015), “Bending and buckling analyses of functionally graded material (FGM) size-dependent nanoscale beams including the thickness stretching effect”, *Steel Compos. Struct*., **18**(2), 425.
Malekzadeh, K., Khalili, S. and Abbaspour, P. (2010), “Vibration of non-ideal simply supported laminated plate on an elastic foundation subjected to in-plane stresses”, *Compos. Struct*., **92**(6), 1478-1484.
Murmu, T. and Pradhan, S. (2009), “Thermo-mechanical vibration of a single-walled carbon nanotube embedded in an elastic medium based on nonlocal elasticity theory”, *Comput. Mater. Sci*., **46**(4), 854-859.
Pakdemirli, M. and Boyac, H. (2001), “Vibrations of a stretched beam with non-ideal boundary”, *Math. Comput. Appl*., **6**(3), 217-220.
Pakdemirli, M. and Boyac, H. (2003), “Non-linear vibrations of a simple–simple beam with a non-ideal support in between”, *J. Sound Vib*., **268**(2), 331-341.
Peddieson, J., Buchanan, G.R. and McNitt, R.P. (2003), “Application of nonlocal continuum models to nanotechnology”, *Int. J. Eng. Sci*., **41**(3), 305-312.
Pradhan, S. and Reddy, G. (2011), “Thermo mechanical buckling analysis of carbon nanotubes on winkler foundation using non-local elasticity theory and DTM”, *Sadhana*, **36**(6), 1009-1019.
Reddy, J. (2007), “Nonlocal theories for bending, buckling and vibration of beams”, *I Int. J. Eng. Sci*., **45**(2), 288-307.
Sari, G. and Pakdemirli, M. (2012), “*Effects of non-ideal boundary conditions on the vibrations of a slightly curved micro beam.* Paper presented at the 9th international conference on mathematical problems in engineering, aerospace and sciences: ICNPAA 2012.
Thai, H.T. (2012), “A nonlocal beam theory for bending, buckling, and vibration of nanobeams”, *Int. J. Eng. Sci*., **52**, 56-64.
Tounsi, A., Bourada, M., Kaci, A. and Houari, M.S.A. (2015), “A new simple shear and normal deformations theory for functionally graded beams”, *Steel Compos. Struct*., **18**(2), 409.

Tounsi, A., Houari, M.S.A. and Benyoucef, S. (2013), "A refined trigonometric shear deformation theory for thermoelastic bending of functionally graded sandwich plates", *Aerosp. Sci. Technol.*, **24**(1), 209-220.
Wang, L., Ni, Q., Li, M. and Qian, Q. (2008), "The thermal effect on vibration and instability of carbon nanotubes conveying fluid", *Physica E: Low-dimensional Systems and Nanostructures*, **40**(10), 3179-3182.
Wang, Q. (2005), "Wave propagation in carbon nanotubes via nonlocal continuum mechanics", *J. Appl. Phys.*, **98**(12), 124301.
Wang, Q., Zhou, G. and Lin, K. (2006), "Scale effect on wave propagation of double-walled carbon nanotubes", *Int. J. Solids Struct.*, **43**(20), 6071-6084.
Wattanasakulpong, N. and Mao, Q. (2015), "Dynamic response of Timoshenko functionally graded beams with classical and non-classical boundary conditions using Chebyshev collocation method", *Compos. Struct.*, **119**, 346-354.
Yahia, S.A., Atmane, H.A., Houari, M.S.A. and Tounsi, A. (2015), "Wave propagation in functionally graded plates with porosities using various higher-order shear deformation plate theories", *Struct. Eng. Mech.*, **53**(6), 1143.
Zemri, A., Houari, M.S.A., Bousahla, A.A. and Tounsi, A. (2015), "A mechanical response of functionally graded nanoscale beam: an assessment of a refined nonlocal shear deformation theory beam theory", *Struct. Eng. Mech.*, **54**(4), 693-710.
Zhang, C.L. and Shen, H.S. (2007), "Buckling and postbuckling of single-walled carbon nanotubes under combined axial compression and torsion in thermal environments", *Phys. Rev. B*, **75**(4), 045408.
Zhang, Y., Liu, G. and Wang, J. (2004), "Small-scale effects on buckling of multiwalled carbon nanotubes under axial compression", *Phys. Rev. B*, **70**(20), 205430.
Zidi, M., Tounsi, A., Houari, M.S.A. and Bég, O.A. (2014), "Bending analysis of FGM plates under hygro-thermo-mechanical loading using a four variable refined plate theory", *Aerosp. Sci. Technol.*, **34**, 24-34.

CC